

# Compromised antigen binding and signaling interfere with bispecific CD19 and CD79a chimeric antigen receptor function

Isabel Leung,<sup>1</sup> Megan L. Templeton,<sup>1</sup> Yun Lo,<sup>1</sup> Anusha Rajan,<sup>1</sup> Sylvia M. Stull,<sup>1</sup> Sarah M. Garrison,<sup>1</sup> Alexander I. Salter,<sup>1</sup> Kimberly S. Smythe,<sup>1</sup> Colin E. Correnti,<sup>1</sup> Shivani Srivastava,<sup>1</sup> Cecilia C. S. Yeung,<sup>1,2</sup> and Stanley R. Riddell<sup>1,3</sup>

<sup>1</sup>Clinical Research Division, Fred Hutchinson Research Center, Seattle, WA; and <sup>2</sup>Department of Pathology, and <sup>3</sup>School of Medicine, University of Washington, Seattle, WA

## Key Points

- Bispecific CAR T cells circumvent outgrowth of antigen-negative tumor cells in vivo.
- Tandem and bicistronic CARs have reduced sensitivity to single-antigen tumor cells because of compromised antigen binding and signaling.

Therapy with CD19-directed chimeric antigen receptor (CAR) T cells has transformed the treatment of advanced B-cell malignancies. However, loss of or low antigen expression can enable tumor escape and limit the duration of responses achieved with CAR T-cell therapy. Engineering bispecific CAR T cells that target 2 tumor antigens could overcome antigen-negative escape. We found that CD79a and b, which are heterodimeric components of the B-cell receptor, were expressed on 84.3% of lymphoma cases using immunohistochemistry, and 87.3% of CD79ab-positive tumors also coexpressed CD19. We generated 3 bispecific permutations: tandem, bicistronic, and pooled products of CD79a-CD19 or CD79b-CD19 CAR T cells and showed that bispecific CAR T cells prevented the outgrowth of antigen-negative cells in a CD19-loss lymphoma xenograft model. However, tandem and bicistronic CAR T cells were less effective than monospecific CD19 or CD79a CAR T cells for the treatment of tumors that only expressed CD19 or CD79, respectively. When compared with monospecific CAR T cells, T cells expressing a tandem CAR exhibited reduced binding of each target antigen, and T cells expressing a bicistronic CAR vector exhibited reduced phosphorylation of downstream CAR signaling molecules. Our study showed that despite added specificity, tandem and bicistronic CAR T cells exhibit different defects that impair recognition of tumor cells expressing a single antigen. Our data provide support for targeting multiple B-cell antigens to improve efficacy and identify areas for improvement in bispecific receptor designs.

## Introduction

The adoptive transfer of genetically modified T cells expressing a CD19-specific chimeric antigen receptor (CAR) is effective for refractory and relapsed B-cell malignancies, resulting in complete response rates up to 93%, 54%, and 67% in acute lymphocytic leukemia (ALL),<sup>1</sup> non-Hodgkin lymphoma<sup>2,3</sup> (NHL), and mantle cell lymphoma (MCL),<sup>4</sup> respectively. However 17% to 61% of patients with NHL and ALL subsequently relapse,<sup>5</sup> and the absence or low expression of CD19 on tumor cells is a major mechanism of escape.<sup>3,6-9</sup>

Human cancers are heterogeneous, and it is unsurprising that targeting a single antigen may not always achieve complete tumor elimination. Simultaneous targeting of multiple B-cell antigens, such as CD19 and CD22 or CD19 and CD20, prevents the outgrowth of CD19-negative variants in preclinical models<sup>10-13</sup> and has shown promise in clinical trials.<sup>9,14-21</sup> However, CD20 and CD22 present

Submitted 14 July 2022; accepted 18 October 2022; prepublished online on *Blood Advances* First Edition 5 December 2022. <https://doi.org/10.1182/bloodadvances.2022008559>.

Data are available on request from the corresponding author, Stanley R. Riddell ([sriddell@fredhutch.org](mailto:sriddell@fredhutch.org)).

The full-text version of this article contains a data supplement.

© 2023 by The American Society of Hematology. Licensed under [Creative Commons Attribution-NonCommercial-NoDerivatives 4.0 International \(CC BY-NC-ND 4.0\)](https://creativecommons.org/licenses/by-nc-nd/4.0/), permitting only noncommercial, nonderivative use with attribution. All other rights reserved.

challenges as CAR targets: CD22 is expressed at variable levels in B-ALL and NHL,<sup>22,23</sup> and high antigen expression is necessary for CAR T-cell recognition.<sup>9,24-26</sup> Moreover, incorporating CD22- and CD19-specific single-chain variable fragments (scFvs) as a tandem single chain has compromised the activity against each target.<sup>27</sup> First-line treatment of NHL includes monoclonal antibody targeting of CD20, and this selective pressure may increase the heterogeneity of CD20 expression on tumor cells.<sup>28,29</sup> Thus, it is important to characterize additional targets in B-cell malignancies and understand the potential limitations of multispecific targeting.

CD79a and CD79b are expressed in early B-cell lymphopoiesis as a heterodimer associated with the surface immunoglobulin.<sup>30,31</sup> CD79ab expression is retained on most CD19-positive B-cell neoplasms,<sup>32-34</sup> making these molecules candidates for multispecific targeting with CARs,<sup>35</sup> bispecific T-cell engagers, or antibody drug conjugates.<sup>36</sup> Indeed, an antibody drug conjugate targeting CD79b is approved for the treatment of diffuse large B-cell lymphoma (DLBCL).<sup>37</sup> We developed CD79a- and CD79b-directed CARs and examined their use in tandem, bicistronic, and pooled bispecific formats combined with a CD19 CAR. Our data demonstrate that bispecific CAR T cells can mitigate antigen loss and that the tandem and bicistronic CD79a-CD19 CAR designs are more effective in tumor clearance than monospecific CAR T cells when both antigens are present on a majority of tumor cells. However, in scenarios where tumor cells express only a single antigen (ie, CD19 or CD79), the function of tandem and bicistronic CAR T cells is compromised compared with the respective monovalent CAR T cells because of less efficient antigen binding and decreased downstream signaling, respectively.

## Methods

### Mouse models

The Fred Hutch Cancer Center (FHCC) institutional animal care and use committee approved all experimental procedures. NSG mice were purchased from Jackson Laboratory or bred in house. Mice (6-8 weeks old) were injected intravenously with JeKo-1, JeKo-1CD19-, or JeKo-1CD79- eGFP-ffluc cells, and cohorts were treated with CD4 and CD8 CAR T or mock T cells mixed at a 1:1 ratio 7 days later. Tumor size was measured by bioluminescence imaging as described.<sup>38</sup> Bone marrow (BM) was isolated from hindlimbs when mice reached euthanasia requirement because of a high tumor burden, followed by red blood cell lysis and staining for flow cytometry.

### Flow cytometry

BM suspensions were stained with LIVE/DEAD Fixable Aqua (ThermoFisher), washed, and stained with fluorochrome-conjugated antibodies in phosphate-buffered saline (PBS) + 2% bovine serum albumin + 3.6 mM EDTA. Antibodies used were anti-human CD45 (2D1), CD79b (C3B-1), CD19 (HIB19), CD20 (2H7), CD22 (HIB22), CD8 (RPA-T8), CD4 (RPA-T4), and EGFR (AY13). Antibodies used in the phenotypic panel were PD1 (eBioJ105), Tim3 (F38-2E2), LAG3 (11C3C65), CD62L (DREG-56), CD25 (BC96), TIGIT (A15153G), and EGFR (AY13). CD79a/b or CD19 CAR staining was performed by incubating cells with recombinant human CD79ab-Fc (rhCD79ab-fc) or rhCD19-biotin, respectively, at 4°C for 20 minutes and staining with antigen-presenting cell-conjugated anti-human Fc (HP6017) or

streptavidin-PE (BioLegend). Tumor cell antibody-binding capacity for CD19 or CD79b were measured using Quantibrite Phycoerythrin Beads (BD Biosciences) and used according to the manufacturer's instructions. Samples were acquired on Fortessa or Celesta flow cytometer (Becton Dickinson).

### CAR T-cell generation

Peripheral blood was obtained from healthy donors following the protocols approved by the FHCC institutional review board. The study was conducted according to the Declaration of Helsinki. CD4 and CD8 T cells were isolated using EasySep CD4<sup>+</sup> and CD8<sup>+</sup> T-cell-negative selection (STEMCELL Technologies), activated, transduced, and cultured as described.<sup>39</sup> Lentiviral vector encoding CD19-specific CAR with 1 STII tag was previously described,<sup>40</sup> CD79 CAR lentiviral vectors were constructed using variable light (V<sub>L</sub>) and variable heavy (V<sub>H</sub>) sequences from US20130089547A1 (CD79a) and WO2016/090210A1, EP2641618A2, US 2007/0207142A1C14, and WO2017/009474A1 (CD79b). Codon-optimized CAR transgenes were synthesized by Thermo Fisher Scientific. Lentivirus was concentrated by mixing with one-fourth volume of 40% polyethylene glycol-8000 overnight at 4°C, centrifuging it at 1800g for 20 minutes, followed by resuspending the pellet in Dulbecco's modified eagle medium, and ultracentrifuging it at 24 500 RPM for 90 minutes at 4°C. Viral pellet was resuspended in Dulbecco's modified eagle medium by vortexing for 2 hours, then stored at -80°C. CAR T cells were enriched based on truncated human epidermal growth factor receptor (EGFRt) expression using fluorescence-activated cell sorting (FACS) or staining with anti-EGFR-biotin, followed by magnetic separation using antibiotin microbeads (Miltenyi Biotec).

### Cell lines

K562, Raji, and JeKo-1 were obtained from the American Type Culture Collection. MAVER-1, NU-DUL-1, RAMOS, SU-DHL-1, OCI-LY1, and Gumbus cells were a gift from Marie Bleakley. GRANTA-519, Daudi, RAMOS, FL-18, and Rec1 were a gift from Brian Till. Tumor lines were cultured in RPMI with 100 U/mL penicillin/streptomycin and 5% FBS. JeKo-1 cells were transduced to express GFP and firefly luciferase. JeKo-1 CD19 or CD79b knockout cells were generated by nucleofection with the Alt-R CRISPR-Cas9 system (Integrated DNA Technologies) using predesigned crRNAs specific for the CD19 or CD79b genes (Integrated DNA Technologies). Briefly, crRNAs were mixed with tracrRNA at equimolar concentrations and annealed by heating to 95°C for 5 minutes, followed by slow cooling to room temperature. crRNA-tracrRNA duplexes were combined and complexed with Cas9 nuclease and electroporation enhancer for 15 minutes. Ribonucleotide protein complexes were mixed with JeKo-1 cells resuspended in SF buffer (Lonza) and electroporated using the 4D Nucleofector (Lonza). CD19<sup>-</sup> or CD79b<sup>-</sup> cells were FACS-sorted at least twice for purity. K562CD19, K562CD79b, or K562CD79ab cells were generated by transducing K562 cells to overexpress CD19, CD79b, or CD79a and b and then FACS-sorted for positivity.

### In vitro assays

Tumor cytotoxicity was measured by chromium release assay as described.<sup>41</sup> Interleukin-2 (IL-2) and interferon gamma (IFN- $\gamma$ ) release was measured in supernatants after coculturing  $2.5 \times 10^4$

CD8 CAR T cells with target cells at 1:1 ratio or with recombinant CD19-biotin or CD79ab-Fc-coated 96-well plates via enzyme-linked immunosorbent assay (Invitrogen). Avi-tagged rhCD19 and rhCD79ab-Fc were produced in house (FHCC). CD19 was biotinylated using the BirA biotinylation kit (Avidity). To coat biotinylated rhCD19 in 96-well plates, 100 mL of avidin (Invitrogen) at 10 mg/mL was incubated overnight in 96-well high-binding plates (Corning). Next day, avidin-coated plates were washed with PBS and blocked with PBS + 2% bovine serum albumin for 1 hour at 4°C. Biotinylated rhCD19 was serially diluted in PBS in low binding plates (Corning), and 100 mL was transferred to blocked avidin plates and incubated for 30 minutes at room temperature. Serially diluted rhCD79ab-Fc was coated by direct adsorption onto 96-well high-binding plates for 20 hours. Plates were washed with PBS and ready for plate-bound stimulation.

### Western blotting

T cells were stimulated by plate-bound antigen in 96 wells. For each condition,  $2 \times 10^5$  T cells were plated per well in 4 to 6 replicates. Plates were centrifuged at 400g for 1 minute and incubated at 37°C for 30 minutes. Plates were placed on ice to arrest signaling, and cells were collected, washed, and lysed with NP40 (Invitrogen) supplemented with HALT™ protease inhibitor (Thermo Fisher Scientific) and phosphatase inhibitor (Thermo Fisher Scientific). An equal amount of protein lysate was loaded into 4% to 15% Mini-PROTEAN gels (Bio-Rad) and transferred onto PVDF using the Trans-Blot Turbo transfer system (Bio-Rad). Membranes were blocked and stained in EveryBlot Blocking Buffer (Bio-Rad). Primary antihuman antibodies were purchased from Cell Signaling unless specified: CD247 (8D3, BD Biosciences), CD247 pTyr142 (K25-407.69, BD Biosciences), PLCγ (D9D6E), PLCγ pTyr783 (D6M9S), SLP76 (D1R1A), SLP76 pSer376 (D9D6E), extracellular signal-regulated kinase (ERK) (137F5), and ERK pThr202/Tyr204 (D13.14.4E).

### Multiplex immunohistochemistry

Protocols for the procurement of human and animal tissues were approved by the institutional review board of the FHCC or obtained as tissue microarrays from US Biomax (LY401 and LY1001d). Formalin-fixed paraffin-embedded tissues were stained on a Leica BOND Rx autostainer using the Akoya Opal Multiplex IHC assay (Akoya Biosciences) with the following changes: additional high-stringency washes were performed after the secondary antibody and Opal fluor applications using high-salt TBST (0.05M Tris, 0.3M NaCl, and 0.1% Tween-20, pH 7.2-7.6). TCT (0.05M Tris, 0.15M NaCl, 0.25% Casein, 0.1% Tween 20, pH 7.6 +/- 0.1) was used as the blocking buffer. All primary antibodies were incubated for 1 hour at room temperature. Antibodies used are listed in Table 1. Slides were mounted with ProLong Gold and cured for 24 hours at room temperature in the dark before image acquisition at 20x magnification on the Akoya Polaris Automated Imaging System. Images were spectrally unmixed using Akoya Phenoptics inForm software. Staining positivity was scored by a board-certified hematopathologist (C.C.S.Y.).

## Results

### CD79 and CD19 are coexpressed on MCL and DLBCL

We investigated CD19 and CD79a or CD79b expression on tumor cell lines using a quantitative antibody-binding assay and on patient

lymphoma samples using immunohistochemistry. Antibody reagents to assess surface CD79a by flow cytometry are unavailable; therefore, we used CD79b surface expression on the tumor cell lines as a surrogate for the CD79ab heterodimer.<sup>42-44</sup> CD79b and CD19 were coexpressed on tumor lines derived from MCL, Burkitt's lymphoma, DLBCL, and follicular lymphoma, whereas some cell lines (Granta, FL18, and Raji) had low levels of CD79b (Figure 1A; supplemental Figure 1A). Analysis of 140 patient tumor specimens using immunohistochemistry identified CD79a and CD79b double-positive expression on 118 (84.3%), CD79a single-positive on 8, and CD79b single-positive on 3 samples. Of the 140 cases, 116 (82.9%) were CD19<sup>+</sup>, and of the CD19<sup>+</sup> cases, 103 (88.8%) were CD79a and b double-positive (Figure 1B; supplemental Figure 1B). These data are consistent with prior reports showing CD79ab expression in most mucosa-associated lymphoid tissue lymphoma, DLBCL, and MCL<sup>32-34,42,45</sup> and support cotargeting of CD19 and CD79a or CD79b by CAR T cells.

### Design of CD79a and CD79b CARs

We generated CD79a and CD79b CARs using 5 different antibody sequences specific for CD79b and 1 for CD79a. The variable chain sequences were positioned in variable light (V<sub>L</sub>)-variable heavy (V<sub>H</sub>) and V<sub>H</sub>-V<sub>L</sub> orientations and linked via spacer sequences to a CD28 transmembrane domain and 4-1BB-CD3ζ signaling domains. A EGFRt transduction marker was included downstream of a T2A ribosomal skip element (Figure 2A). A long immunoglobulin G spacer with mutations to prevent Fc receptor binding<sup>38</sup> was chosen because the short ectodomains of the CD79 molecules predicted a longer spacer would provide optimal CAR T-cell engagement with the tumor cell.<sup>46</sup> Initial studies optimizing the CD79b-specific A17v14b scFv showed the superiority of a CAR with the long spacer compared with a short immunoglobulin G hinge spacer format (supplemental Figure 2A-C).

T cells expressing similar levels of EGFRt and each of the CARs were evaluated for binding to recombinant CD79ab-Fc protein. Target binding of individual CARs was variable, with CD79a 9G6, CD79b 2F2, and CD79b 4450 CARs demonstrating the highest binding (supplemental Figure 3A). T cells expressing 9G6, 2F2, and 4450 CARs, each constructed in the V<sub>L</sub>V<sub>H</sub> orientation, exhibited superior cytokine production and tumor lysis compared with those designed in the V<sub>H</sub>V<sub>L</sub> format and to other CD79b scFvs (supplemental Figure 3B-C). Based on these data, 9G6 (CD79a) and 2F2 (CD79b) CARs in the V<sub>L</sub>V<sub>H</sub> monospecific format were selected for in vivo studies and for the design of bispecific formats.

### CAR T-cell treatment results in antigen loss in an MCL xenograft model

We compared the antitumor activity of CD79a, CD79b, and CD19 monospecific CAR T cells in vitro and in vivo using a xenograft model of human MCL (JeKo-1). CD79a and CD79b CAR T cells lysed tumor lines with comparable potency to CD19 CAR T cells (Figure 2B). CD79b CAR T cells produced similar levels of IL-2 and IFN-γ as CD19 CAR T cells after tumor stimulation; however, CD79a CAR T cells produced lower levels of cytokines, and this difference was significant for IFN-γ with 2 of the 4 tumor lines (Figure 2C). In mice engrafted with JeKo-1 cells, monospecific CD79a or CD79b CAR T cells controlled tumors and extended survival compared with untreated mice but were less effective than CD19 CAR T cells (Figure 2D-E). Analysis of the BM identified

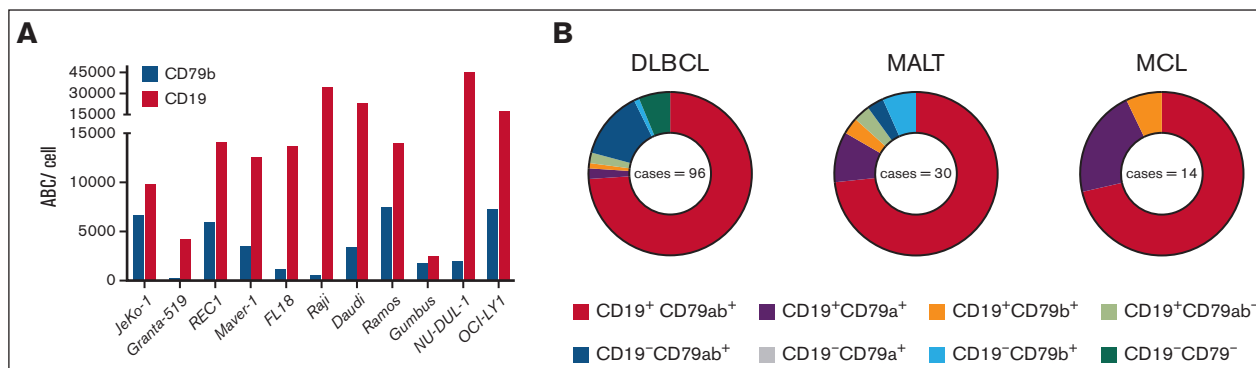


**Figure 1. CD79ab is expressed on lymphoma cell lines and primary tumor specimens.** (A) CD19 and CD79b density on each indicated tumor cell line measured via ABC. (B) Expression of CD19, CD79a, and CD79b measured by IHC on primary lymphoma specimens. ABC, antibody-binding capacity; Burkitt's, Burkitt's lymphoma; FL, follicular lymphoma; MALT, lymphoma of the mucosa-associated lymphoid tissue.

CD4<sup>+</sup> and CD8<sup>+</sup> CAR T cells in all treatment groups and showed that persisting JeKo-1 tumor in mice treated with CD79a or CD79b CAR T cells exhibited complete loss of CD79b (Figure 2F; supplemental Figure 4A). CD19 loss was also observed in some mice with persisting tumor after CD19 CAR T cells (Figure 2F; supplemental Figure 4A). Thus, monospecific CD79a, CD79b, or CD19 CAR T cells have *in vivo* activity, but targeting a single antigen allowed the outgrowth of antigen-negative tumor cells at varying rates. It is notable that CD79b loss on a small minority of JeKo-1 cells was seen in some untreated mice and in mice treated with CD19 CAR and coincided with lower expression of CD22 and CD20 (supplemental Figure 4A-B). This loss of B-lineage markers is consistent with plasmacytic differentiation of JeKo-1 *in vivo*, which has been reported in other B-cell malignancies.<sup>47-49</sup> Because plasmacytic differentiation is rare, targeting multiple B-lineage antigens may be beneficial for most patients.

### Design of bispecific CARs

We then examined dual targeting of CD19 and CD79a or CD79b with T cells expressing a tandem CAR, bicistronic CARs, or by pooling monospecific CAR T cells (Figure 3A). Tandem CD79a-19 and tandem CD79b-19 encoded CD79a or b and CD19-specific scFvs separated by a linker in a single molecule, with the CD79a or b scFv placed in the membrane distal position. Bicistronic CD19-79a and bicistronic CD19-79b, expressed 2 distinct CAR proteins encoded by a single lentivirus. CAR expression and tumor recognition *in vitro* were identical to those of monospecific CAR T cells and were not affected by the order in which the CAR-coding sequences were positioned (supplemental Figure 5A-D). Constructs with the CD19 CAR sequence positioned upstream of the CD79a or b CAR sequences were selected for further study (Figure 3A). Finally, the pooled product consisted of a combination of 2 monospecific CAR T cells mixed at a 1:1 ratio.

All bispecific CAR products lysed tumor cells *in vitro* at comparable efficiency to monospecific CAR T cells and produced IL-2 and IFN- $\gamma$  against both CD79ab<sup>+</sup>CD19<sup>+</sup> JeKo-1 cells and K562 cells expressing either CD19 or CD79ab (Figure 3B-C). We observed no differences in activation, differentiation, or exhaustion markers in unstimulated bispecific compared with monospecific CAR T cells, consistent with the absence of tonic signaling (supplemental Figure 6).

### Bispecific CAR T cells prevent antigen loss and prolong survival in a CD19 antigen escape model

Because the outgrowth of CD19-negative JeKo-1 was delayed in NSG mice, we created a CD19-loss variant of JeKo-1 using gene editing (supplemental Figure 7) and engrafted mice with a mixture of 99% wild-type (CD19<sup>+</sup>CD79ab<sup>+</sup>) and 1% JeKo-1<sup>CD19KO</sup> cells. Cohorts of mice were then treated with CD19 CAR T cells or with each of the CD79a/b-CD19 bispecific CAR T-cell products. As expected, treatment with CD19 CAR T cells alone resulted in the outgrowth of CD19<sup>-</sup> tumor cells over 4 to 5 weeks (Figure 4A). In contrast, mice treated with the same dose of CAR T cells expressing tandem, bicistronic, or pooled CAR T-cell products targeting CD79a or CD79b and CD19 exhibited improved tumor control and survival relative to the CD19 CAR T-cell-treated group (Figure 4B-C). The data showed a trend toward better tumor control with tandem and bicistronic CAR T cells cotargeting CD79a and CD19, as compared with the respective CD79b-CD19 bispecific CAR T cells (Figure 4B). In contrast to CD19 CAR T-treated mice, where all persisting tumor cells in the BM were CD19-negative, most of the tumor cells that persisted after treatment with bispecific CAR T cells maintained CD79b and CD19 expression (Figure 4D). Thus, low bispecific CAR T-cell doses prevented relapse with a CD19<sup>-</sup> tumor.

### Tandem and bicistronic CAR formats are superior to CD19 CAR T cells in controlling JeKo-1 tumors but show compromised activity against JeKo-1 that only expressed CD19 or CD79a

We focused on the CD79a-CD19 bispecific CARs because they were more effective than the CD79b-CD19 bispecifics in the CD19 escape model. We evaluated the potency of tandem CD79a-CD19 and bicistronic CD19-CD79a CAR T cells, the pooled CD19:CD79a T-cell product, and monospecific CD19 CAR T cells in mice engrafted with wild-type JeKo-1 tumor cells. Mice were treated with a subcurative dose of monospecific CD19 CAR T cells or an identical dose of each of the various CD79a-CD19 CAR T-cell products. Our results showed improved tumor control and prolonged survival in mice treated with tandem CD79a-19 and bicistronic CD19-79a CAR T cells compared with CD19 CAR T cells (Figure 5A-B). Tumor outgrowth and survival with the pooled product mirrored that of monospecific CD19 CAR T-cell



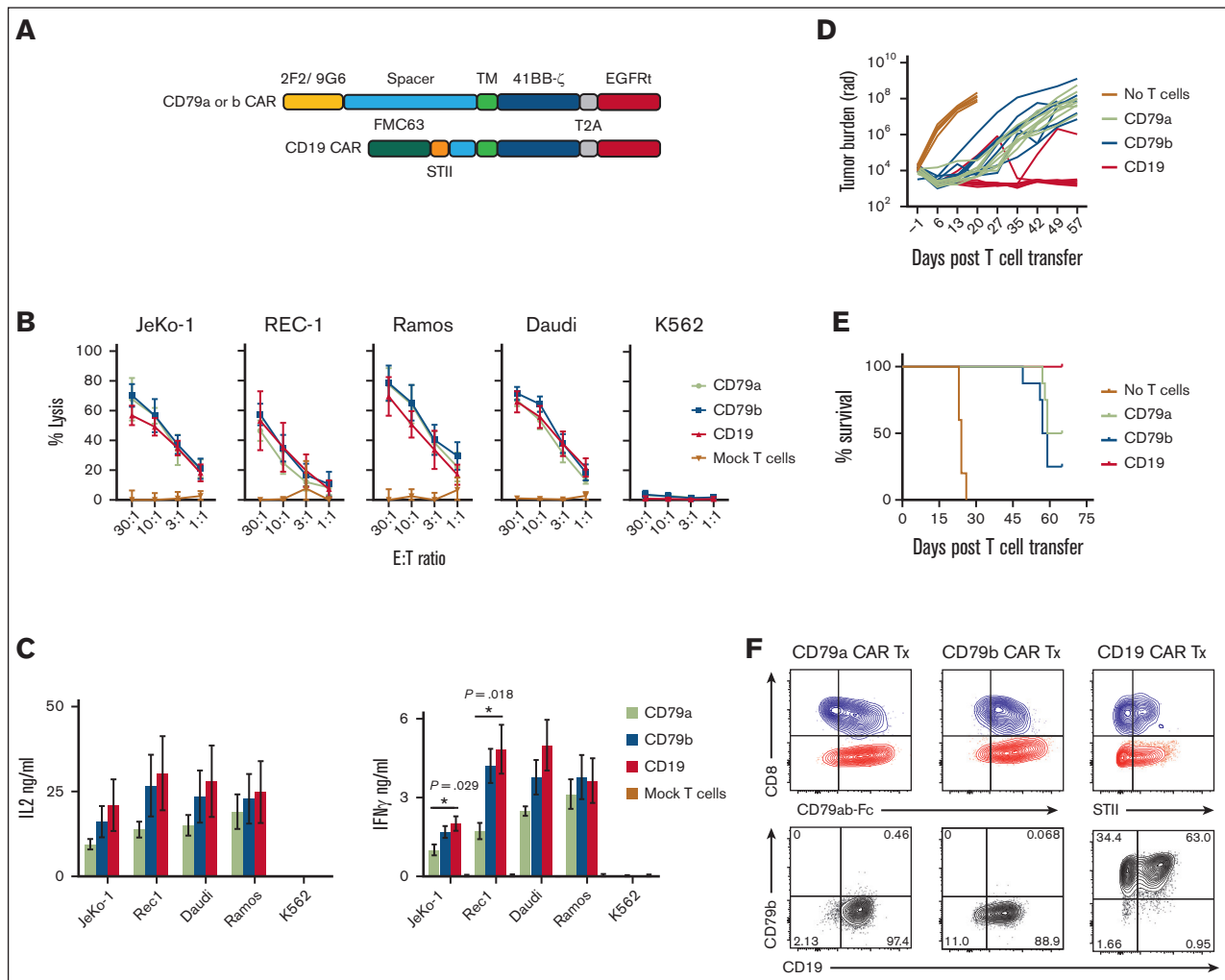


**Figure 2. CD79a and CD79b CAR T cells are functional in vitro and in vivo.** (A) Schematic of CD19, CD79a, or CD79b CAR constructs. (B) Lysis of indicated tumor cell lines by chromium release assay. Data are means  $\pm$  SEM from 3 independent experiments. (C) CAR T-cell IL-2 or IFN- $\gamma$  production measured by ELISA. Data are means  $\pm$  SEM from 4 independent experiments. *P* values were calculated with one-way ANOVA with post hoc Tukey multiple comparisons test. (D-E) NSG mice were inoculated with JeKo-1 ffluc tumor cells and either left untreated or treated at day 7 with a total of  $2 \times 10^6$  of CD79a, CD79b, or CD19 CAR T cells (CD4:CD8 at 1:1 ratio). (D) Bioluminescent imaging of tumor bearing mice at indicated time points. Each line represents measurements of a single mouse in each of the treatment groups. (E) Survival of mice from 2 independent experiments, each containing 5 to 8 mice per group. (F) Representative flow cytometric analysis of T cells and tumor cells in BM suspensions from JeKo-1 tumor bearing mice treated with CD79a, CD79b, or CD19 CAR T cells on the day that mice met criteria for euthanasia. Top panels were gated on singlets, live cells, and CD45<sup>+</sup>CD8<sup>+</sup> (blue) or CD45<sup>+</sup>CD4<sup>+</sup> (red) population. CAR staining was measured by CD79ab-Fc or anti-STII antibody binding. Bottom panels were gated on singlets, live cells, and CD45<sup>+</sup>GFP<sup>+</sup> JeKo-1 ffluc cells. ANOVA, analysis of variance; ELISA, enzyme-linked immunosorbent assay; SEM, standard error of the mean; TM, transmembrane domain.

treatment, which is consistent with published reports that pooled CAR T products targeting other receptors are less effective in vivo than tandem or bicistronic CAR designs.<sup>12,50</sup> What underlies the superior potency of bispecific vs pooled monospecific products is unclear but may relate to heightened avidity for tumor cells of T cells expressing tandem or bicistronic CARs because of higher total tumor antigen density (ie, CD79a and CD19).

Tandem and bicistronic CAR T cells had improved tumor control compared with CD19 CAR T cells when most tumor cells coexpressed CD79 and CD19. However, cytokine production by mono- and bispecific CAR T cells after stimulation with immobilized CD19 or CD79ab recombinant proteins showed that the maximal amount of

IL-2 and IFN- $\gamma$  produced was lower for tandem and bicistronic CD79a-CD19 CAR T cells compared with monospecific CAR T cells, suggesting recognition of tumors expressing only a single antigen where avidity gains would be abrogated might be compromised (Figure 5C-D). To examine whether the in vitro functional defects affected the efficacy against tumor cells expressing only a single antigen in vivo, we compared tumor control mediated by tandem and bicistronic CD79a-CD19 products to monospecific CD19 or CD79a CAR T cells in mice engrafted with JeKo-1 cells that expressed only CD19 or CD79ab (supplemental Figure 7). In mice engrafted with JeKo-1<sup>CD19KO</sup> cells, we observed that CD79a-directed tumor control mediated by tandem and bicistronic products was less effective compared with monospecific CD79a CAR T cells (Figure 5E-F). In

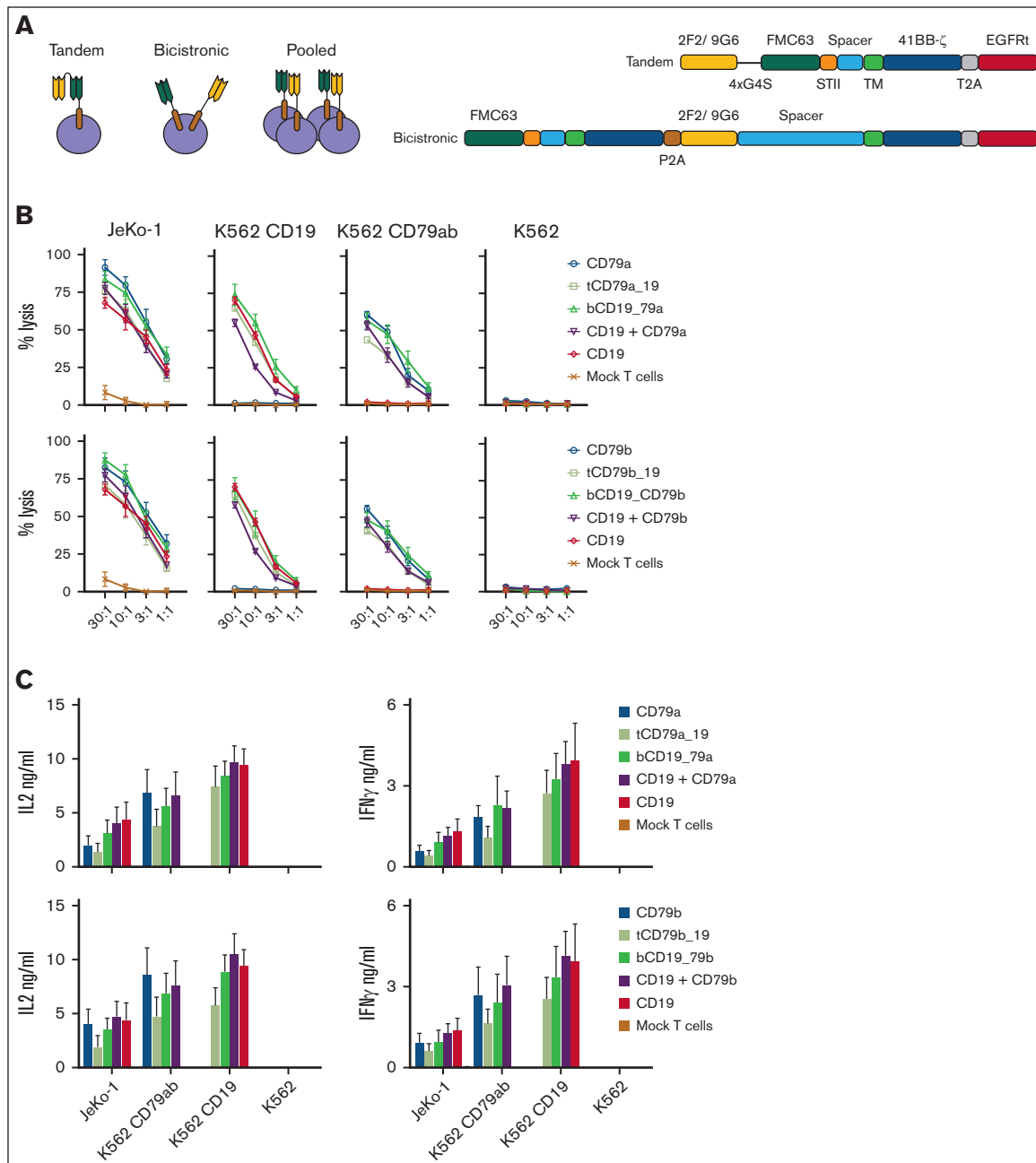


**Figure 3. Design and in vitro characterization of bispecific CARs.** (A) Schematics of bispecific CAR T-cell formats. (B) Top panels: lysis of the indicated tumor cell lines by CD19, CD79a, and bispecific CD79a-CD19 CAR T cells. tCD79a-CD19 refers to tandem CAR; bCD19-CD79a refers to bicistrionic CAR. Bottom panel: lysis of the indicated tumor cell lines by CD19, CD79b, and bispecific CD79b-CD19 CAR T cells. tCD79b-CD19 refers to tandem CAR; bCD19-CD79b refers to bicistrionic CAR. (C) CAR T-cell IL-2 and IFN- $\gamma$  production measured by ELISA. Data given in (A-B) are means  $\pm$  SEM from 3 independent experiments. ELISA, enzyme-linked immunosorbent assay; SEM, standard error of the mean.

addition, mice engrafted with CD79<sup>-</sup> tumors (JeKo-1<sup>CD79KO</sup>) and treated with tandem CAR T cells showed reduced survival compared with mice treated with bicistrionic CD19-CD79a and monospecific CD19 CAR T cells (Figure 5G-H). Although bicistrionic CAR T cells had reduced cytokine production in response to CD19 antigen in vitro (Figure 5D), tumor control and survival were comparable to CD19 CAR T cells (Figure 5G-H), perhaps because of the contributions of other tumor cell-surface molecules that facilitate recognition by CAR T cells.

### Tandem CD79a-19 CAR has reduced binding for CD19 and CD79ab than the monospecific or bicistrionic CARs

To determine if CAR expression was comparable in T cells expressing monospecific and bispecific CARs, we stained the Strep-tag II incorporated upstream of the hinge in the monospecific, tandem, and bicistrionic CD19 CAR (Figures 2A and 3A). STII staining showed that the tandem CAR and the bicistrionic

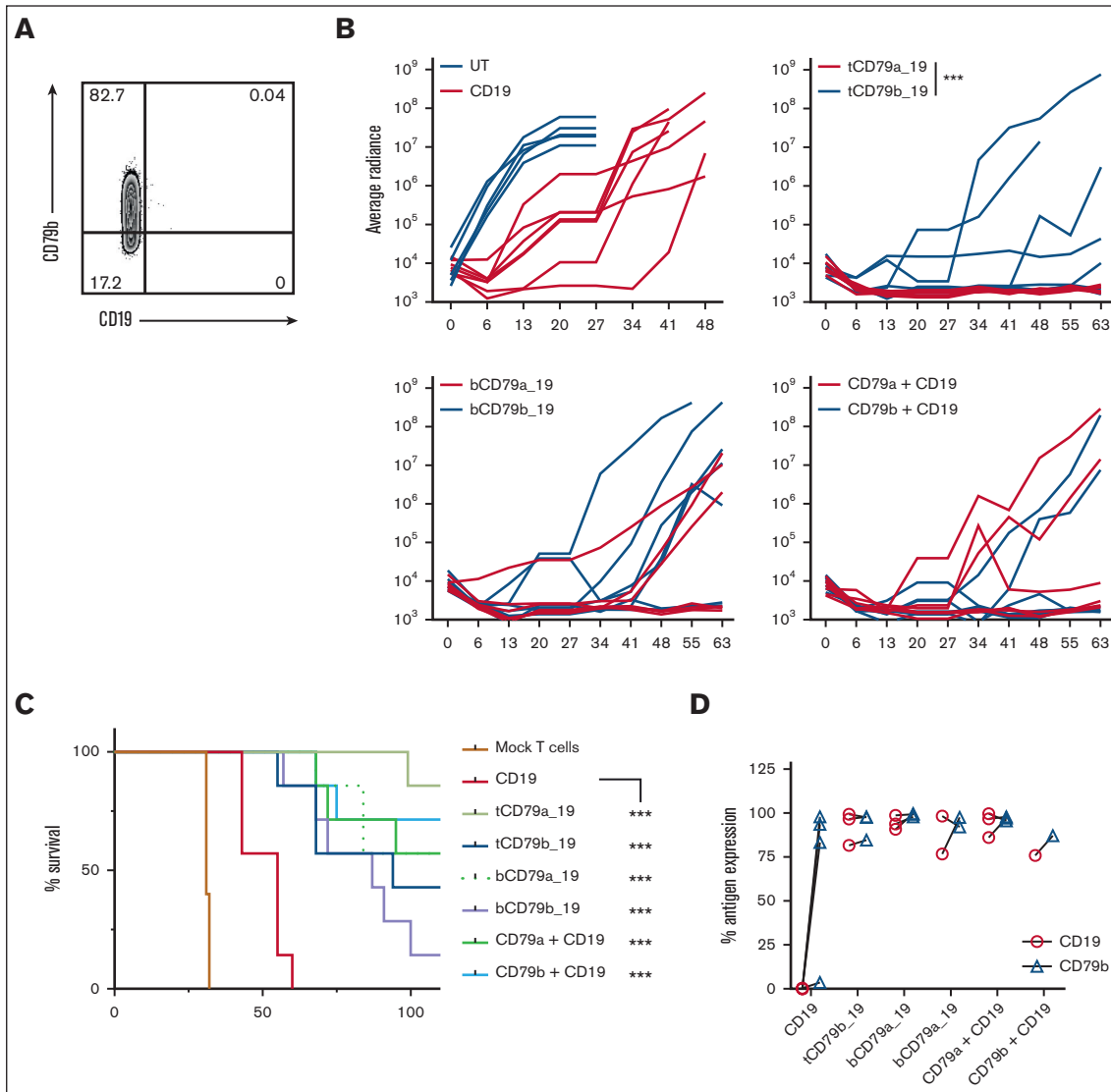


**Figure 4. Bispecific CAR T cells prevent antigen loss in a CD19 escape xenograft model.** (A) Representative flow plot of BM tumor cells from mice treated CD19 CAR T cells in the CD19 escape model. (B) Bioluminescent imaging of mice engrafted with 99% JeKo-1<sup>wt</sup> + 1% JeKo-1<sup>CD19KO</sup> cells and then treated with  $0.6 \times 10^6$  of the indicated CAR T cells or mock-transduced T cells (CD4:CD8 at 1:1 ratio). \*\*\* $P \leq .001$  with a  $q \leq 0.01$  on day 41 was calculated using multiple Mann-Whitney  $t$  test. (C) Survival of mice in each treatment group shown in panel B. (D) Quantification of CD79b or CD19 expression measured by flow cytometry on BM tumor cells from mice in each treatment group. For panel B, \*\*\* $P \leq .001$  was calculated with log-rank (Mantel-Cox) test. Data shown were pooled from 2 independent experiments with a total of 5 (mock) or 7 mice per group.

CD19 CAR were expressed at levels comparable with the CD19 CAR (Figure 6A). Despite equivalent CAR expression, binding of recombinant CD19 and CD79ab proteins by the tandem CD79a-CD19 CAR T cells was reduced relative to CD19 monospecific or bicistronic CD19-CD79a CAR T cells (Figure 6A). It is not surprising that antigen binding was unaffected in the bicistronic design because the CD19 CAR and the CD79a CAR on both monospecific and bicistronic CAR T cells have identical CAR structures and expression. In contrast, recombinant CD79ab protein binding was reduced for tandem CD79a-CD19 CAR T cells compared with monospecific CD79a CAR T cells (Figure 6A). We expressed an N-terminal MYC tag on both the monospecific CD79a CAR and the tandem CAR to address whether differences in CAR expression might explain the lower level of CD79ab

binding. The tandem CD79a-CD19 CAR was expressed at a slightly lower level than the CD79a CAR; however, when CAR expression was normalized by gating on CAR T cells with equivalent levels of MYC, CD79ab binding was still reduced significantly (Figure 6B). The reduction in CD19 and CD79ab binding in the tandem format could be due to steric hindrance or destabilization of the scFv structure by linkage of the scFvs, as has been observed in bispecific antibody formats.<sup>51,52</sup>

### Bicistronic CAR format compromises downstream signaling

We next sought an explanation for the reduced activation of T cells expressing the bicistronic CAR and the less effective control of

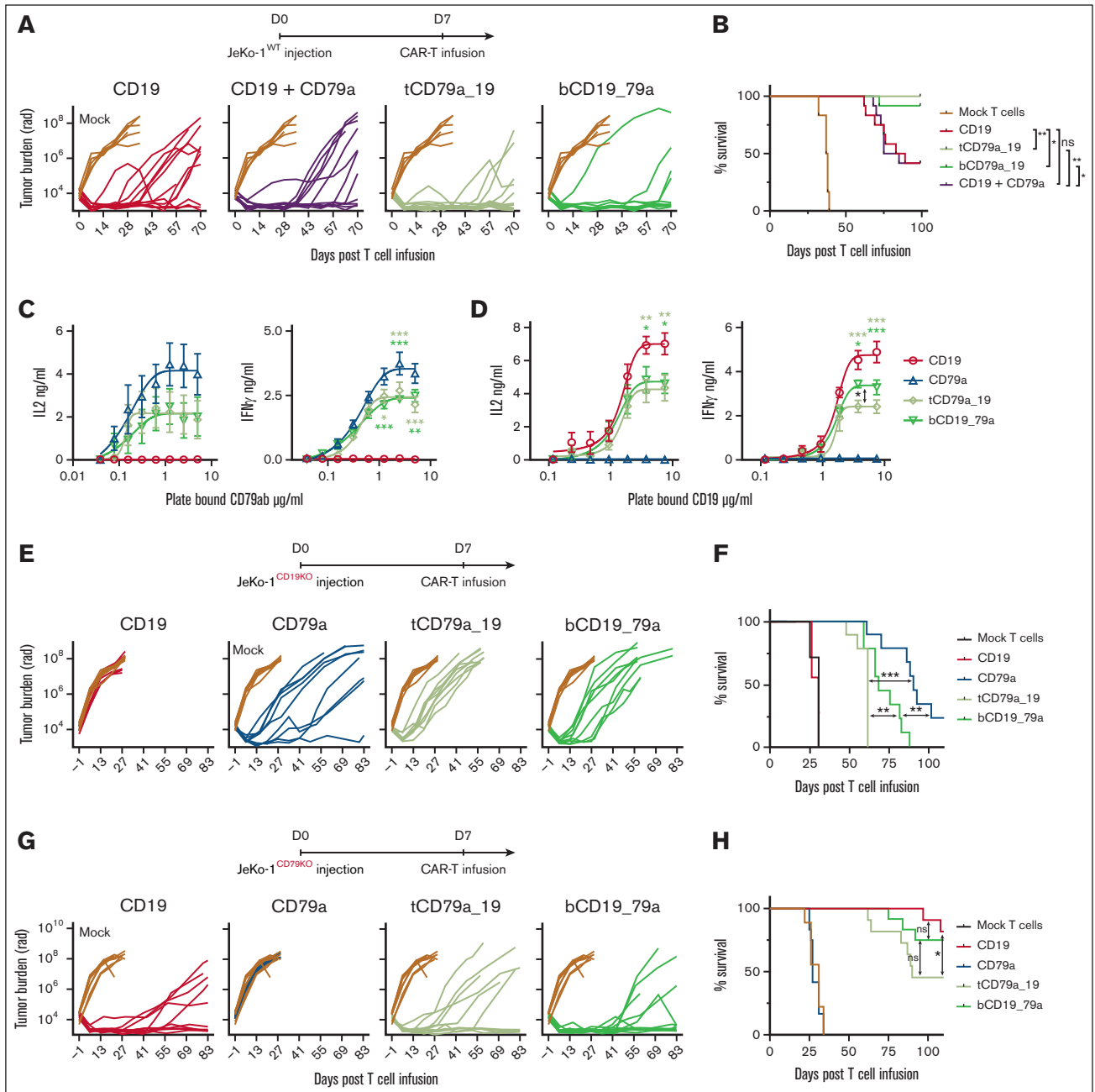


**Figure 5. Treatment of mice engrafted with wild-type JeKo-1 and single antigen expressing JeKo-1 with tandem, bicentric, and monospecific CD79a and CD19 CAR T cells.** (A-B) Cohorts of JeKo-1 tumor bearing NSG mice were treated with  $0.6 \times 10^6$  of mock-transduced T cells, CD19, tandem CD79a-19, bicistrionic CD19-79a, or CD19 + CD79a CAR T cells (CD4:CD8 at 1:1 ratio). Data were pooled from 2 independent experiments consisting of a total of 6 to 12 mice per group. (A) Bioluminescent imaging of tumor bearing mice at indicated time points. Each line represents measurements in a single mouse. (B) Survival of mice in each treatment group. (C-D) IL-2 and IFN- $\gamma$  production measured by ELISA of supernatants harvested 20 hours after coculture of CAR T cells on plate-bound CD79ab-Fc or (D) plate-bound CD19. Data given are means  $\pm$  SEM from 3 independent experiments done with different donors. (E-F) Cohorts of NSG mice engrafted with JeKo-1<sup>CD19KO</sup> or JeKo-1<sup>CD79KO</sup> were either treated with  $0.6 \times 10^6$  of mock-transduced T cells, CD19, CD79a, tandem CD79a-19, or bicistrionic CD19-79a CAR T cells (CD4:CD8 at 1:1 ratio). (E) Bioluminescent imaging of tumor bearing mice at indicated time points. Each line represents measurements in a single mouse. (F) Survival of mice in each treatment group. Data were pooled from 2 or 3 experiments with 7, 9, 11, or 12 mice per group. \*\*\* $P \leq .001$ , \*\* $P \leq .01$  and \* $P \leq .05$ , were calculated with panel B, and panel F Log-rank (Mantel-Cox) test, panels C-D, two-way ANOVA. Asterisks are color matched to the bispecific CAR to reflect the comparison between the indicated bispecific CAR and the monospecific CD79a CAR in panel C or CD19 CAR in panel D.



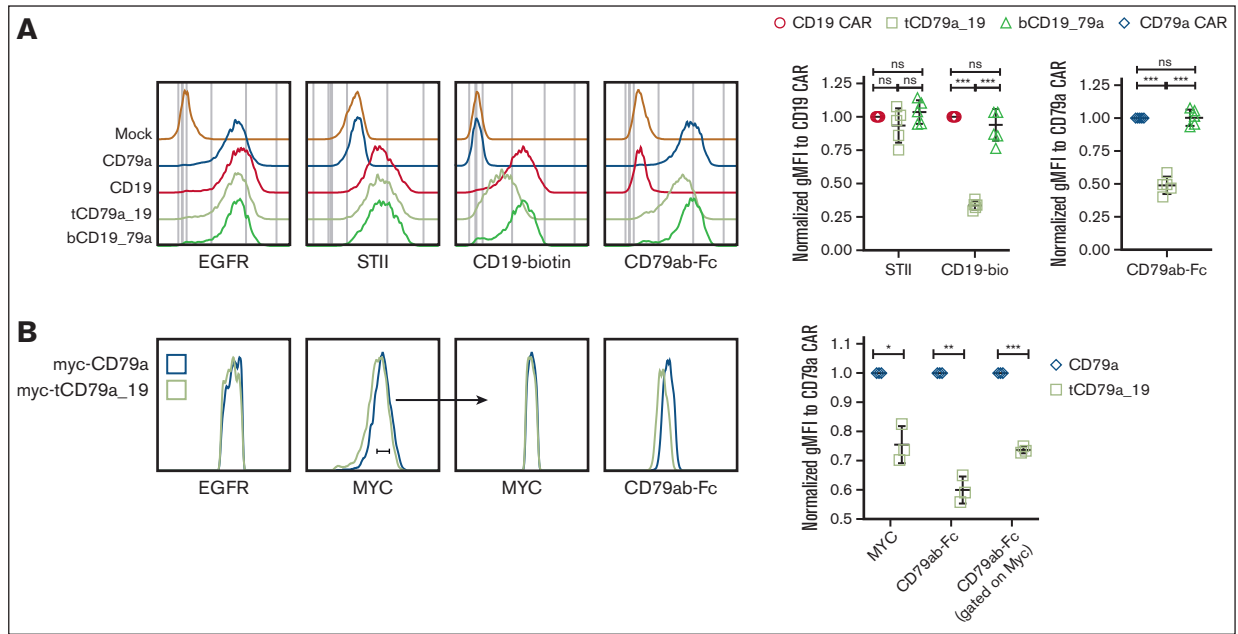


**Figure 6. Tandem CAR design has impaired antigen binding compared with the monospecific CARs.** (A) CAR expression determined by flow cytometry staining with anti-STII, CD19-biotin, and CD79ab-Fc staining on sorted EGFR+ T cells. Right panels show quantification of normalized gMFI determined from flow cytometric staining of 5 different donors. Quantification was normalized to the mean obtained by staining monospecific CD19 CAR T cells with anti-STII or CD19-biotin binding. Quantification for CD79ab-Fc binding was normalized to that obtained with the monospecific CD79a CAR. (B) Flow cytometric histograms of indicated CAR T cells gated on EGFR+ cells, showing anti-MYC or CD79ab-Fc staining. Right panel shows quantification of normalized gMFI flow cytometric staining of 3 different donors. Quantification was normalized to CD79a CAR T cell for anti-MYC or CD79ab-Fc binding for each donor. Indicated *P* values were with \*\*\**P* < .001, \*\**P* < .01, \**P* < .05 or ns were calculated with one-way ANOVA Tukey multiple comparisons test and panel B paired *t* test. ns, not significant.

CD19-CD79ab<sup>+</sup> tumor cells in vivo (Figure 5C-D). Because bicistronic CAR T cells have a higher total number of surface CARs compared with monospecific CAR T cells, we hypothesized that competition for intracellular signaling molecules might limit the quality of signaling through each receptor, particularly against tumor cells expressing a single antigen where only 1 of the 2 receptors is

engaged. Indeed, phosphorylation of key signaling molecules, including CAR CD3 $\zeta$ , SLP76, PLC $\gamma$ , and ERK was reduced after stimulation with plate-bound CD19 or CD79ab compared with monospecific CARs (Figure 7A-B). Thus, despite equivalent expression, signaling through 1 CAR in a bicistronic CAR T cell is compromised compared with a monospecific CAR T cell.

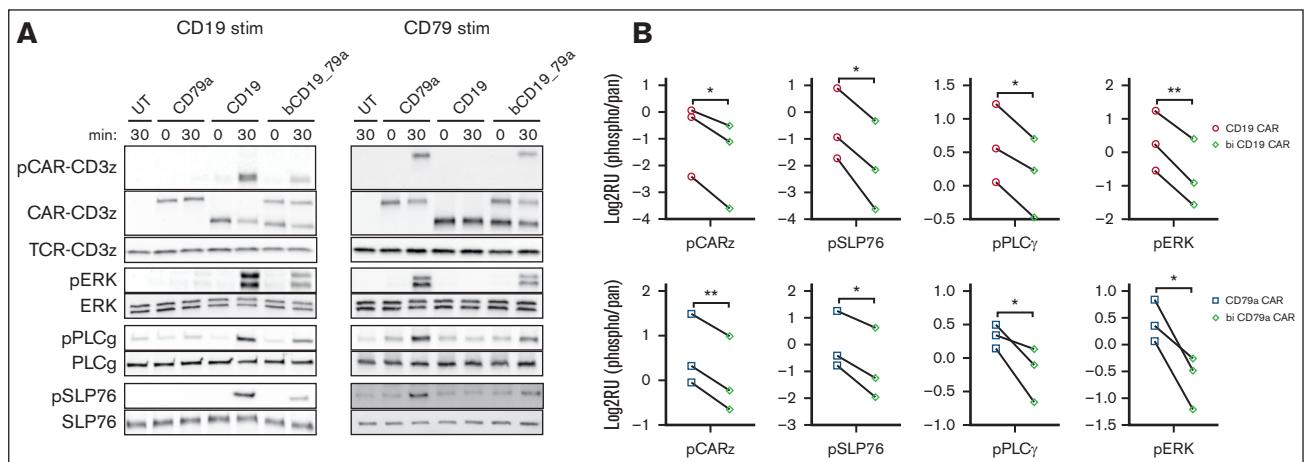


**Figure 7. Bicistronic CAR T cells have reduced phosphorylation of CD3 $\zeta$  and downstream signaling molecules compared with monospecific CAR T cells, after stimulation.** (A) Western blots showing levels of phosphorylated and total protein for the indicated analytes from monospecific CD79a, CD19, and bicistronic CD19-79a CAR T cells at baseline (0 minute) and 30 minutes after stimulation by immobilized CD19 or CD79ab recombinant protein. (B) Log<sub>2</sub> values of normalized band intensities measured by densitometry from 3 independent experiments. \*\**P* < .01 and \**P* < .05 were calculated with paired two-tailed *t* test.

**Table 1. Antibodies used in multiplexed immunohistochemistry**

Position	Antibody	Clone/host	Company/item	Concentration $\mu\text{g/mL}$	OPAL fluor
1	CD3	SP7 / rabbit	Thermo Fisher Scientific / RM-9107	0.06 (1:400)	520
2	CD19	UMAB103 / mouse	Origene / UM500071	0.5 (1:2000)	690
3	CD33	RBT-CD33 / rabbit	Bio SB Inc / BSB3451	1 (1:100)	570
4	CD79A	JCB117 / mouse	Bio SB Inc / BSB5305	0.166 (1:600)	540
5	CD79B	EPR6861 / rabbit	Abcam / ab134147	0.065 (1:1600)	620
6	Cyclin-D	SP4 / rabbit	Sigma / SAB5500090	0.625 (1:400)	650
Secondary	Opal polymer HRP Ms+Rb		Akoya Biosciences / ARH1001EA	Ready to use	

## Discussion

Targeting multiple antigens is presently viewed as an attractive strategy to prevent the outgrowth of antigen-low or antigen-negative tumor cells, which has been widely documented in clinical trials of monospecific CAR T cells.<sup>1,23,53-59</sup> However, the potential limitations of various strategies for multiantigen targeting have not been elucidated.<sup>9,14,17,60-62</sup> To fill these knowledge gaps, we examined the strengths and limitations of targeting CD19 and CD79a in tandem, bispecific, and pooled CAR T-cell formats. CD79a-CD19 tandem and bicistronic designs were effective in preventing the outgrowth of antigen-negative tumor cells and performed better than a monospecific CD19 CAR in a lymphoma model. However, deficiencies in current bispecific CAR designs were identified that affected their ability to control tumor cells that were positive for only 1 of the target antigens.

Our tandem construct targeting CD79a and CD19 exhibited reduced avidity for binding each of the targeted antigens, which was likely due to steric hindrance or protein instability caused by fusion of 2 independent scFvs. This reduction in antigen sensitivity coincided with compromised function against tumor cells expressing only CD19 or CD79a in vivo. A recent clinical trial showed that a fraction of relapsed patients treated with a tandem CD19-CD22 CAR had persistence of tumor cells that were CD19-negative or -low but had preserved CD22 expression, suggesting that the CD22 targeting was compromised in their tandem design.<sup>9</sup> Another clinical study using a different tandem CD19-CD22 CAR structure reported 1 of 3 patient relapses had CD19-negative tumor cells with diminished CD22 expression.<sup>15</sup> These clinical studies suggest that the current iterations of bispecific CAR designs might not be equipped to fully address antigen loss. In addition, a tandem multitargeting CAR comprising designed ankyrin repeat proteins rather than scFvs also showed that the tandem CAR was not as effective as monospecific CARs against tumor cells expressing only 1 antigen.<sup>63</sup> Thus, loss in antigen sensitivity could be prevalent in tandem CAR designs and should be investigated in future designs and for different cancer targets. It is conceivable that using alternative linkers connecting the antigen-binding domains guided by structural predictions,<sup>64</sup> or scFvs with higher affinity, may improve the antigen sensitivity of tandem constructs.

An alternative to tandem CARs is to express each receptor in a bicistronic format to preserve the monospecific CAR architecture. Although CD19 and CD79a bicistronic CARs were expressed and bound CD19 and CD79 equivalently to monospecific CARs, our data show that these receptors are impaired in downstream signaling. Although the exact mechanism for reduced CAR signaling is unknown, it has been previously shown that CARs exhibit basal signaling and assemble an interactome of signaling

molecules.<sup>65</sup> Thus, 1 possible explanation is that the higher total number of CAR molecules in the bicistronic design could result in competition for signaling proteins that associate with the CAR and compromise the quality of signaling when the CAR engages an antigen. Further studies using quantitative techniques such as mass spectrometry to analyze the proteins that are complexed to monospecific and bicistronic CARs might identify signaling proteins that are reduced because of competition, as a study showed that CAR/TCR signaling proteins may be limited and shared among the 2 complexes in a T cell.<sup>66</sup> These issues reveal that our molecular understanding of CAR function, particularly in bispecific formats, remains incomplete, and further understanding may help address clinical shortcomings where antigen escape continues to be observed in tandem<sup>9,15</sup> and bicistronic<sup>60</sup> CAR T-cell therapy trials.

Our preclinical study identified that tandem and bicistronic designs were better than monospecific CARs in MCL antigen loss or MCL xenograft models but were less effective than monospecific CARs at treating tumors that were either CD19- or CD79-positive. Thus, the added benefit of dual specificity occurred at the expense of less sensitivity toward each target antigen. This raises the question of how effective these formats will be at treating cancers that are highly heterogenous, where a significant fraction of tumor cells are positive for only 1 of the targeted antigens. Clinical trials using tandem and bicistronic CAR T cells may shed light on this issue.

## Acknowledgments

This work was funded by National Institutes of Health grants CA18029 and CA224536 and the Leukemia and Lymphoma Society.

## Authorship

Contribution: I.L. and S.R.R. designed research, analyzed data, and wrote the manuscript; I.L., M.L.T., Y.L., A.R., S.M.S., S.M.G., and K.S.S. performed experiments; A.I.S. and C.E.C. designed reagents; S.S. provided scientific input; and C.C.S.Y. provided pathology analysis.

Conflict-of-interest disclosure: S.R.R. is a cofounder of Lyell Immunopharma; has received grant funding and has intellectual property licensed to Lyell Immunopharma; was a founder of Juno Therapeutics, a Bristol Myers Squibb company; and has served as a scientific adviser to Juno Therapeutics and Adaptive Biotechnologies. The remaining authors declare no competing financial interests.

The current affiliation for C.E.C. is Link Immunotherapeutics, Seattle, WA.

## References

1. Maude SL, Laetsch TW, Buechner J, et al. Tisagenlecleucel in children and young adults with B-cell lymphoblastic leukemia. *N Engl J Med*. 2018; 378(5):439-448.
2. Locke FL, Ghobadi A, Jacobson CA, et al. Long-term safety and activity of axicabtagene ciloleucel in refractory large B-cell lymphoma (ZUMA-1): a single-arm, multicentre, phase 1-2 trial. *Lancet Oncol*. 2019;20(1):31-42.
3. Neelapu SS, Locke FL, Bartlett NL, et al. Axicabtagene ciloleucel CAR T-cell therapy in refractory large B-cell lymphoma. *N Engl J Med*. 2017;377(26): 2531-2544.
4. Wang M, Munoz J, Goy A, et al. KTE-X19 CAR T-cell therapy in relapsed or refractory mantle-cell lymphoma. *N Engl J Med*. 2020;382(14):1331-1342.
5. Majzner RG, Mackall CL. Clinical lessons learned from the first leg of the CAR T cell journey. *Nat Med*. 2019;25(9):1341-1355.
6. Yu H, Sotillo E, Harrington C, et al. Repeated loss of target surface antigen after immunotherapy in primary mediastinal large B cell lymphoma. *Am J Hematol*. 2017;92(1):E11-E13.
7. Shalabi H, Kraft IL, Wang HW, et al. Sequential loss of tumor surface antigens following chimeric antigen receptor T-cell therapies in diffuse large B-cell lymphoma. *Haematologica*. 2018;103(5):e215-e218.
8. Brudno JN, Shi V, Stroncek D, et al. T cells expressing a novel fully-human anti-CD19 chimeric antigen receptor induce remissions of advanced lymphoma in a First-in-Humans Clinical Trial. *Blood*. 2016;128(22):999.
9. Spiegel JY, Patel S, Muffly L, et al. CAR T cells with dual targeting of CD19 and CD22 in adult patients with recurrent or refractory B cell malignancies: a phase 1 trial. *Nat Med*. 2021;27(8):1419-1431.
10. Schneider D, Xiong Y, Wu D, et al. A tandem CD19/CD20 CAR lentiviral vector drives on-target and off-target antigen modulation in leukemia cell lines. *J Immunother Cancer*. 2017;5:42.
11. Zah E, Lin MY, Silva-Benedict A, Jensen MC, Chen YY. T cells expressing CD19/CD20 bispecific chimeric antigen receptors prevent antigen escape by malignant B cells. *Cancer Immunol Res*. 2016;4(6):498-508.
12. Ruella M, Barrett DM, Kenderian SS, et al. Dual CD19 and CD123 targeting prevents antigen-loss relapses after CD19-directed immunotherapies. *J Clin Invest*. 2016;126(10):3814-3826.
13. Fousek K, Watanabe J, Joseph SK, et al. CAR T-cells that target acute B-lineage leukemia irrespective of CD19 expression. *Leukemia*. 2021;35(1): 75-89.
14. Schultz LM, Muffly LS, Spiegel JY, et al. Phase I trial using CD19/CD22 bispecific CAR T cells in pediatric and adult acute lymphoblastic leukemia (ALL). *Blood*. 2019;134(suppl 1):744.
15. Dai H, Wu Z, Jia H, et al. Bispecific CAR-T cells targeting both CD19 and CD22 for therapy of adults with relapsed or refractory B cell acute lymphoblastic leukemia. *J Hematol Oncol*. 2020;13(1):30.
16. Pan J, Zuo S, Deng B, et al. Sequential CD19-22 CAR T therapy induces sustained remission in children with r/r B-ALL. *Blood*. 2020;135(5):387-391.
17. Shah NN, Johnson BD, Schneider D, et al. Bispecific anti-CD20, anti-CD19 CAR T cells for relapsed B cell malignancies: a phase 1 dose escalation and expansion trial. *Nat Med*. 2020;26(10):1569-1575.
18. Tong C, Zhang Y, Liu Y, et al. Optimized tandem CD19/CD20 CAR-engineered T cells in refractory/relapsed B-cell lymphoma. *Blood*. 2020;136(14): 1632-1644.
19. Amrolia PJ, Wynn R, Hough RE, et al. Phase I study of AUTO3, a bicistronic chimeric antigen receptor (CAR) T-cell therapy targeting CD19 and CD22, in pediatric patients with relapsed/refractory B-cell acute lymphoblastic leukemia (r/r B-ALL): Amelia study. *Blood*. 2019;134(suppl 1):2620.
20. Sang W, Shi M, Yang J, et al. Combination of anti-CD19 and anti-CD20 chimeric antigen receptor T cells for relapsed and refractory diffuse larger B cell lymphoma: an open-label, single-arm, phase I/II trial. *Blood*. 2019;134(suppl 1):1590.
21. Wang N, Hu X, Cao W, et al. Efficacy and safety of CAR19/22 T-cell cocktail therapy in patients with refractory/relapsed B-cell malignancies. *Blood*. 2020;135(1):17-27.
22. Rosenthal J, Naqvi AS, Luo M, et al. Heterogeneity of surface CD19 and CD22 expression in B lymphoblastic leukemia. *Am J Hematol*. 2018;93(11): E352-E355.
23. Fry TJ, Shah N, Orentas R, et al. CD22-targeted CAR T cells induce remission in B-ALL that is naive or resistant to CD19-targeted CAR immunotherapy. *Nat Med*. 2018;24(1):20-28.
24. Haso W, Lee DW, Shah NN, et al. Anti-CD22-chimeric antigen receptors targeting B-cell precursor acute lymphoblastic leukemia. *Blood*. 2013;121(7): 1165-1174.
25. Majzner RG, Rietberg SP, Sotillo E, et al. Tuning the antigen density requirement for CAR T-cell activity. *Cancer Discov*. 2020;10(5):702-723.

26. Ramakrishna S, Highfill SL, Walsh Z, et al. Modulation of target antigen density improves CAR T-cell functionality and persistence. *Clin Cancer Res*. 2019;25(17):5329-5341.
27. Qin H, Ramakrishna S, Nguyen S, et al. Preclinical development of bivalent chimeric antigen receptors targeting both CD19 and CD22. *Mol Ther Oncolytics*. 2018;11:127-137.
28. Duman BB, Sahin B, Ergin M, Guvenç B. Loss of CD20 antigen expression after rituximab therapy of CD20 positive B cell lymphoma (diffuse large B cell extranodal marginal zone lymphoma combination): a case report and review of the literature. *Med Oncol*. 2012;29(2):1223-1226.
29. Smith MR. Rituximab (monoclonal anti-CD20 antibody): mechanisms of action and resistance. *Oncogene*. 2003;22(47):7359-7368.
30. Reth M. Antigen receptors on B lymphocytes. *Annu Rev Immunol*. 1992;10:97-121.
31. Dworzak MN, Fritsch G, Froschl G, Printz D, Gadner H. Four-color flow cytometric investigation of terminal deoxynucleotidyl transferase-positive lymphoid precursors in pediatric bone marrow: CD79a expression precedes CD19 in early B-cell ontogeny. *Blood*. 1998;92(9):3203-3209.
32. Myklebust JH, Brody J, Kohrt HE, et al. Distinct patterns of B-cell receptor signaling in non-Hodgkin lymphomas identified by single-cell profiling. *Blood*. 2017;129(6):759-770.
33. Cabezudo E, Carrara P, Morilla R, Matutes E. Quantitative analysis of CD79b, CD5 and CD19 in mature B-cell lymphoproliferative disorders. *Haematologica*. 1999;84(5):413-418.
34. Chu PG, Loera S, Huang Q, Weiss LM. Lineage determination of CD20- B-Cell neoplasms: an immunohistochemical study. *Am J Clin Pathol*. 2006;126(4):534-544.
35. Ormhoj M, Scarfò I, Cabral ML, et al. Chimeric antigen receptor T cells targeting CD79b show efficacy in lymphoma with or without cotargeting CD19. *Clin Cancer Res*. 2019;25(23):7046-7057.
36. Palanca-Wessels MC, Czuczman M, Salles G, et al. Safety and activity of the anti-CD79B antibody-drug conjugate polatuzumab vedotin in relapsed or refractory B-cell non-Hodgkin lymphoma and chronic lymphocytic leukaemia: a phase 1 study. *Lancet Oncol*. 2015;16(6):704-715.
37. Deeks ED. Polatuzumab vedotin: first global approval. *Drugs*. 2019;79(13):1467-1475.
38. Hudecek M, Sommermeyer D, Kosasih PL, et al. The nonsignaling extracellular spacer domain of chimeric antigen receptors is decisive for in vivo antitumor activity. *Cancer Immunol Res*. 2015;3(2):125-135.
39. Salter AI, Ivey RG, Kennedy JJ, et al. Phosphoproteomic analysis of chimeric antigen receptor signaling reveals kinetic and quantitative differences that affect cell function. *Sci Signal*. 2018;11(544).
40. Liu L, Sommermeyer D, Cabanov A, et al. Inclusion of Strep-tag II in design of antigen receptors for T-cell immunotherapy. *Nat Biotechnol*. 2016;34(4):430-434.
41. Hudecek M, Lupo-Stanghellini MT, Kosasih PL, et al. Receptor affinity and extracellular domain modifications affect tumor recognition by ROR1-specific chimeric antigen receptor T cells. *Clin Cancer Res*. 2013;19(12):3153-3164.
42. Mason DY, Cordell JL, Brown MH, et al. CD79a: a novel marker for B-cell neoplasms in routinely processed tissue samples. *Blood*. 1995;86(4):1453-1459.
43. Chu PG, Arber DA. CD79: a review. *Appl Immunohistochem Mol Morphol*. 2001;9(2):97-106.
44. Van Noesel C, Van Lier R. Architecture of the human B-cell antigen receptors. *Blood*. 1993;82(2):363-373.
45. Pfeifer M, Zheng B, Erdmann T, et al. Anti-CD22 and anti-CD79B antibody drug conjugates are active in different molecular diffuse large B-cell lymphoma subtypes. *Leukemia*. 2015;29(7):1578-1586.
46. James SE, Greenberg PD, Jensen MC, et al. Antigen sensitivity of CD22-specific chimeric TCR is modulated by target epitope distance from the cell membrane. *J Immunol*. 2008;180(10):7028-7038.
47. Perez-Galan P, Mora-Jensen H, Weniger MA, et al. Bortezomib resistance in mantle cell lymphoma is associated with plasmacytic differentiation. *Blood*. 2011;117(2):542-552.
48. Gradowski JF, Jaffe ES, Warnke RA, et al. Follicular lymphomas with plasmacytic differentiation include two subtypes. *Mod Pathol*. 2010;23(1):71-79.
49. Ribera-Cortada I, Martinez D, Amador V, et al. Plasma cell and terminal B-cell differentiation in mantle cell lymphoma mainly occur in the SOX11-negative subtype. *Mod Pathol*. 2015;28(11):1435-1447.
50. Hegde M, Mukherjee M, Grada Z, Tandem CAR, et al. T cells targeting HER2 and IL13R $\alpha$ 2 mitigate tumor antigen escape. *J Clin Invest*. 2016;126(8):3036-3052.
51. Yazaki PJ, Lee B, Channappa D, et al. A series of anti-CEA/anti-DOTA bispecific antibody formats evaluated for pre-targeting: comparison of tumor uptake and blood clearance. *Protein Eng Des Sel*. 2013;26(3):187-193.
52. Wu C, Ying H, Grinnell C, et al. Simultaneous targeting of multiple disease mediators by a dual-variable-domain immunoglobulin. *Nat Biotechnol*. 2007;25(11):1290-1297.
53. Maude SL, Frey N, Shaw PA, et al. Chimeric antigen receptor T cells for sustained remissions in leukemia. *N Engl J Med*. 2014;371(16):1507-1517.
54. Gardner R, Wu D, Cherian S, et al. Acquisition of a CD19-negative myeloid phenotype allows immune escape of MLL-rearranged B-ALL from CD19 CAR-T-cell therapy. *Blood*. 2016;127(20):2406-2410.
55. Park JH, Rivière I, Gonen M, et al. Long-term follow-up of CD19 CAR therapy in acute lymphoblastic leukemia. *N Engl J Med*. 2018;378(5):449-459.

56. Turtle CJ, Hanafi LA, Berger C, et al. CD19 CAR-T cells of defined CD4+:CD8+ composition in adult B cell ALL patients. *J Clin Invest*. 2016;126(6):2123-2138.
57. Da Via MC, Dietrich O, Truger M, et al. Homozygous BCMA gene deletion in response to anti-BCMA CAR T cells in a patient with multiple myeloma. *Nat Med*. 2021;27(4):616-619.
58. Samur MK, Fulciniti M, Aktas Samur A, et al. Biallelic loss of BCMA as a resistance mechanism to CAR T cell therapy in a patient with multiple myeloma. *Nat Commun*. 2021;12(1):868.
59. Mikkilineni L, Manasanch EE, Lam N, et al. T cells expressing an anti-B-cell maturation antigen (BCMA) chimeric antigen receptor with a fully-human heavy-chain-only antigen recognition domain induce remissions in patients with relapsed multiple myeloma. *Blood*. 2019;134(suppl 1):3230.
60. Cordoba S, Onuoha S, Thomas S, et al. CAR T cells with dual targeting of CD19 and CD22 in pediatric and young adult patients with relapsed or refractory B cell acute lymphoblastic leukemia: a phase 1 trial. *Nat Med*. 2021;27(10):1797-1805.
61. Fernández de Larrea C, Staehr M, Lopez AV, et al. Defining an optimal dual-targeted CAR T-cell therapy approach simultaneously targeting BCMA and GPRC5D to prevent BCMA escape-driven relapse in multiple myeloma. *Blood Cancer Discov*. 2020;1(2):146-154.
62. Zah E, Nam E, Bhuvan V, et al. Systematically optimized BCMA/CS1 bispecific CAR-T cells robustly control heterogeneous multiple myeloma. *Nat Commun*. 2020;11(1):2283.
63. Balakrishnan A, Rajan A, Salter AI, et al. Multispecific targeting with synthetic ankyrin repeat motif chimeric antigen receptors. *Clin Cancer Res*. 2019;25(24):7506-7516.
64. Jumper J, Evans R, Pritzel A, et al. Highly accurate protein structure prediction with AlphaFold. *Nature*. 2021;596(7873):583-589.
65. Ramello MC, Benzaïd I, Kuenzi BM, et al. An immunoproteomic approach to characterize the CAR interactome and signalosome. *Sci Signal*. 2019;12(568).
66. Salter AI, Rajan A, Kennedy JJ, et al. Comparative analysis of TCR and CAR signaling informs CAR designs with superior antigen sensitivity and in vivo function. *Sci Signal*. 2021;14(697).